Received: 16 July 2019 | Revised: 21 September 2019 | Accepted: 8 October 2019

DOI: 10.1002/aoc.5317

Applied Organometallic Chemistry WILEY

FULL PAPER

Synthesis of new α-aminophosphonates using nanoscale nickel-based metal–organic framework as a heterogeneous catalyst and their antibacterial activity

Sarika A. Rasal[1] | **Pratik P. Dhavan**[2] | **Bhaskar L. Jadhav**[2] | **Navinchandra G. Shimpi**[1]

[1]Laboratory for Material Science, Department of Chemistry, University of Mumbai, Santacruz (E), Mumbai, 400098,, India

[2]Department of Life Sciences, University of Mumbai, Santacruz (E), Mumbai, 400098,, India

Correspondence
Navinchandra G. Shimpi, Laboratory for Material Science, Department of Chemistry, University of Mumbai, Santacruz (E), Mumbai 400098, India.
Email: navin_shimpi@rediffmail.com

Funding information
DST-PURSE

Abstract

An elegant approach was presented for the synthesis of novel α-aminophosphonates: a three-component one-pot condensation of 3-(trifluoromethyl)aniline, substituted aromatic aldehydes, and diethyl phosphite using a nickel-based metal–organic framework (Ni-MOF). The Ni-MOF was synthesized using 4,4′-biphenyldicarboxylic acid and further characterized using various techniques such as X-ray diffraction, Fourier-transform infrared, thermogravimetry/differential thermal analysis, Brunauer–Emmett–Teller, and field-emission scanning electron microscopy analyses. Ni-MOF seems to be an eco-friendly, an easily recyclable, and heterogeneous catalyst up to the eighth run with minimal reduction in its catalytic activity. The synthesized α-aminophosphonates were also investigated for antibacterial and antioxidant activities. In few cases, compounds **4a–4x** show similar as well as higher antibacterial activity. Among the synthesized α-aminophosphonates, **4a–4x** had more potent antibacterial activity against pathogenic bacteria while compounds **4h, 4m, 4n, 4q, 4u, 4v, and 4w** exhibited significant antioxidant activity.

KEYWORDS

antibacterial activity, antioxidant activity, catalysis, metal–organic framework, α-Aminophosphonates

1 | INTRODUCTION

Metal–organic frameworks (MOFs) are the combination of organic and inorganic chemistry whose structure is defined by a three-dimensional arrangement of metal ions or clusters coordinated to bipodal or multipodal organic ligands.[1–3] Mainly, varieties of metal such as alkaline, alkaline earth, transition metals, and rare earth metals have been used in the preparation of MOFs.[4] MOFs have attracted great attention in various applications, such as gas storage/separation/adsorption, biomedicine, molecular-based magnetism, drug delivery, and sensors, due to their characteristic properties (porosity, crystallinity, specific surface area, low density, and relatively strong metal–ligand coordination bond).[5–10]

The most significant application of MOFs is in heterogeneous catalysis.[11] The catalytic activity of MOFs depends on active sites such as metal centers and organic linkers. The area of MOFs has become one of the fastest growing fields in catalysis because of their structural and functional tunability. The activity of MOFs is focused on

several features such as the use of commercial MOFs as a catalyst in comparison with other porous solids or their activity to promote organic transformation reactions (carbon–carbon and carbon-heteroatom bond formation).[12,13] The increase in the length of organic linkers increases pore dimension as well as surface area, which leads to smaller size[14] and eventually to the formation of nanoscale MOFs. These materials provide the features similar to or even more than nanomaterials.[15]

The Kabachnik–Fields reaction is a versatile reaction for the formation of carbon–phosphorus bonds.[16,17] Many natural and synthetic aminophosphonic acid and ester derivatives display a wide range of biological properties such as antimicrobial,[18] antioxidant,[19] anti-inflammatory,[20] antitumor,[21] and insecticidal activities[22] and also act as enzyme inhibitors.[23] Owing to their biological importance, different routes have been developed for the synthesis of aminophosphonate using various starting materials.[24] Recently, our research group has synthesized novel α-aminophosphonates using different substituted aldehydes and amines.[25] The investigation of new α-aminophosphonates thus remains an attractive area of all synthetic organic chemists. This has led to a rapidly expanding interest in exploring their properties and uses.

The literature describes very few studies on nickel-based MOF (Ni-MOF) as catalysts for organic transformation reactions. Kim and co-workers prepared nickel nanoparticles embedded in MOFs for hydrogenation,[26] while Chou and co-workers used MOF-5-supported nickel nanoparticles as a catalyst for hydrogenation of crotonaldehyde.[27] Jiang and co-workers utilized nickel (salphen)-based MOF for CO_2 absorption and *in situ* asymmetric fixation.[28] Canivet and co-workers anchored a nickel complex into a mesoporous MOF to generate an active and reusable catalyst, which was used in the liquid-phase ethylene dimerization to selectively form 1-butene.[29] Truong and co-workers synthesized $Ni_2(BDC)_2(DABCO)$ as a catalyst for oxidative coupling of alkynes and arylboronic acids.[30] Zuo and co-workers used N-doped mesoporous carbon–supported Ni nanoparticles for the reduction of nitroarenes.[31] Moreover, Aryanejad and co-workers investigated novel Ni-MOF as a catalyst for benzyl alcohol oxidation and cascade reaction.[15]

In continuation of our study toward the synthesis of novel α-aminophosphonates, we herein present a simple and expeditious synthesis of α-aminophosphonates using an Ni-MOF as a heterogeneous catalyst under solvent-free conditions. To our knowledge, there are no reports on the synthesis of α-aminophosphonate using 3-(trifluoromethyl)aniline as amine in the presence of Ni-MOF as a catalyst. A series of novel α-aminophosphonates were screened *in vitro* for antibacterial (resazurin microtiter assay [REMA] method) and antioxidant (2,2-diphenyl-1-picrylhydrazyl [DPPH] method) activities. The results obtained revealed that α-aminophosphonates (**4a–4x**) have good to excellent antibacterial and antioxidant activities.

2 | EXPERIMENTAL

2.1 | Materials and characterization

All reagents and starting materials were used as received without further purification (Sigma-Aldrich and Merck, India). The crystalline nature of Ni-MOF was analyzed using powder X-ray diffractometer (Maxima 7000 S; Shimadzu, USA) using Cu-Kα (λ = 1.5418 Å and 1.6-kW X-ray tube with an applied voltage of 40 kV and current values of 40 mA) radiation with 2θ range from 5° to 70° at a scanning speed of 5° min^{-1}. Thermogravimetric analysis was performed from 30 to 800 °C at a heating rate 10 °C/min under an inert atmosphere (METTLER TOLEDO STAR^e System, India). Brunauer–Emmett–Teller (BET) specific surface area and pore dimension were calculated by performing N_2 adsorption–desorption measurements at 77 K. Surface morphology was studied using field-emission scanning electron microscopy (FESEM; Hitachi S-4800, Japan). Ni-MOF was prepared under ultrasonic irradiation, which was achieved using a multiwave ultrasonic cell crusher (SJIA-250w equipped with a converter/transducer and titanium oscillator horn). Thin-layer chromatography was performed using Merck silica gel 60 F_{254} plates and components were visualized under UV light (254 nm). Isolated products were confirmed using Fourier transform infrared (FTIR) spectroscopy (Perkin Elmer, Frontier equipment) under attenuated total reflectance. ^{1}H nuclear magnetic resonance (NMR; 300 Hz) and ^{13}C NMR (75 Hz) were recorded on an NMR spectrometer (Bruker ADVANCE II) using tetramethylsilane as an internal standard and a gas chromatography (GC)–mass spectrometry (MS) spectrometer (QP-2010, Rtx-17, 30 m × 0.25 mm ID, film thickness *df* = 0.25 μm, column flow 2 mL/min, 80–240 °C at 10 °C/min rise). Elemental analysis was performed on a CHNS–O analyzer (EA300, EuroVector, Italy). The *in vitro* antibacterial activity of all the synthesized compounds was investigated using the REMA plate method to obtain minimum inhibitory concentration (MIC) in comparison with chloramphenicol as a standard drug. The antioxidant activity was verified by the DPPH scavenging method with ascorbic acid as a standard.

2.2 | General procedure for preparation of Ni-MOF

Ni-MOF was synthesized according to a previously reported method but with certain modifications.[32] Nickel(II) chloride and 4,4′-biphenyldicarboxylic acid (BPDC) were used to coordinate with nickel ions in order to form Ni-MOFs. For this purpose, initially, the nickel(II) chloride solution (3.72 mmol) was prepared in 100 mL deionized water (DW) and the BPDC solution (4.75 mmol) was prepared in 100 mL DW. The pH of the organic linker solution was adjusted to 7 by dropwise addition of 1 M NaOH solution. Nickel chloride solution was then added dropwise into the organic linker solution under controlled ultrasound conditions for 3 hr. The obtained green precipitate was filtered and washed with DW in excess and further three times using ethanol. The precipitate was dried in a hot air oven at 100 °C for 24 hr.

2.3 | General procedure for the synthesis of α-aminophosphonates

A mixture of aldehyde **(1)** (1 mmol), 3-(trifluoromethyl) aniline **(2)** (1 mmol), diethyl phosphite **(3)** (1.2 mmol), and catalyst (10 mg) were added into a 50-mL round-bottomed flask under controlled stirring at room temperature. The progress of the reaction path was monitored by thin-layer chromatography. After completion of the reaction, ethyl acetate was added to the reaction mixture and the catalyst was removed by centrifugation. The separated catalyst was washed using ethanol and dried in an oven at 80 °C for 24 hr. The organic layer was washed using excess of brine and dried over anhydrous sodium sulphate. Finally, the organic layer was concentrated and the crude product was crystallized to obtain pure α-aminophosphonate (Scheme 1).

2.4 | Protocol for antibacterial activity

The antibacterial activity of synthesized compounds **(4a–4x)** was screened against two Gram-positive bacteria (*Staphylococcus aureus* [ATCC 25923], *Bacillus subtilis* [ATCC 6633]) and Gram-negative bacteria (*Salmonella typhi* [ATCC 23564], *Escherichia coli* [ATCC 25922]) by the REMA.[33] The bacterial suspension was prepared in nutrient broth from test organisms, subcultured on nutrient agar, and incubated at 37 °C for 16 hr. All compounds were dissolved in dimethyl sulfoxide (DMSO) and further diluted with water to prepare the working solution of 1000 μg/mL concentration. Twofold serial dilutions were prepared using a multichannel pipette such that each well has 50 μL of the test material in a series with descending concentrations. Chloramphenicol was used as a positive control (standard drug) and DMSO as a negative control. The microtiter plates were then sealed with parafilm and incubated at 37 °C for 24 hr. After incubation, resazurin (50 μL, 0.2 mg/mL dissolved in sterilized distilled water) was added to each well and plates were incubated again at 37 °C for 30 min. The change in color from purple to pink was assessed visually. The lowest concentration at which color change occurred was taken as the MIC value.

2.5 | Protocol for antioxidant activity

The DPPH radical scavenging activity assay is one of the standard methods used for evaluation of antioxidant activity of compounds.[34–36] The synthesized compounds **(4a–4x)** were tested for antioxidant activity by observing their interaction with the stable free radical DPPH[37,38] using the ascorbic acid as standard. In the following assay, 0.1 mL of 15, 30, 60, 120, and 240 μg/mL of each test compound, 0.8 mL of DPPH, and 0.1 mL of methanol were added into a test tube. The absorbance of each solution was determined at 517 nm using a spectrophotometer after incubation at 37 °C for 30 min. Similarly, absorbance was recorded for control (i.e. methanol and DPPH). The DPPH scavenging ability was calculated using following equation:

$$\text{DPPH scavenging ability}\,(\%) = \frac{\text{Ac} - \text{As}}{\text{Ac}} \times 100 \quad (1)$$

where Ac is absorbance of control; and As is absorbance of sample.

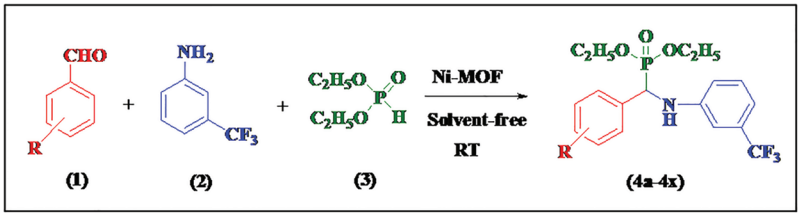

SCHEME 1 Synthesis of α-aminophosphonate. Ni-MOF, nickel-based metal–organic framework; RT, room temperature

3 | RESULTS AND DISCUSSION

3.1 | Characterization of Ni-MOF

The X-ray diffraction (XRD) pattern of Ni-MOF was compared with organic linker to evaluate the formation of Ni-MOF (Figure 1). The appearance of new diffraction peaks of Ni-MOF at 5.6, 12.9, 18.6, 20.5, and 25.7° in comparison with the organic linker (BPDC) can be observed. The XRD pattern of Ni-MOF signifies its highly crystalline nature. The Debye–Scherrer formula was used to calculate the average crystallite size, which was found to be approximately 93 nm.

Figure 2 shows FTIR spectra of Ni-MOF and BPDC. A significant spectral shift of the carboxylate group of Ni-MOF and BPDC confirms the coordination of ligand to metal. In Ni-MOF, the band at 3300 cm^{-1} is assigned to the stretching vibration of coordinated water molecules and peaks at 1598, 1494, and 1430 cm^{-1} are attributed to the C=C stretching mode, which confirms the presence of the aromatic ring. There are two strong bands at 1569 and 1393 cm^{-1}, which are assigned to the asymmetric and symmetric vibrations of the carboxylate groups, respectively. Besides, Ni-MOF shows two intense bands at 682 and 769 cm^{-1}, which indicate the C–H antiplane bending mode of the aromatic ring. The carboxylate group coordinates with the metal center through the bidentate mode, which is confirmed by the difference between the asymmetric and symmetric vibration bands ($\Delta\nu$).

The thermogravimetry/differential thermal analysis (TG-DTA) was performed from 30 to 800 °C at a heating rate 10 °C/min under an inert atmosphere for the investigation of thermal stability of Ni-MOF (Figure 3). The recorded curve showed two separate weight loss steps: a first weight loss (16.58%) from 30 to 250 °C, which can be ascribed to the loss of adsorbed and the trapped moisture inside the framework. Another weight loss (41.69%) at 400 to 600 °C which is due to the decomposition of the organic linker.

The surface area and pore dimensions of Ni-MOF were evaluated by standard nitrogen adsorption–desorption measurements carried out at 77 K. Figure 4

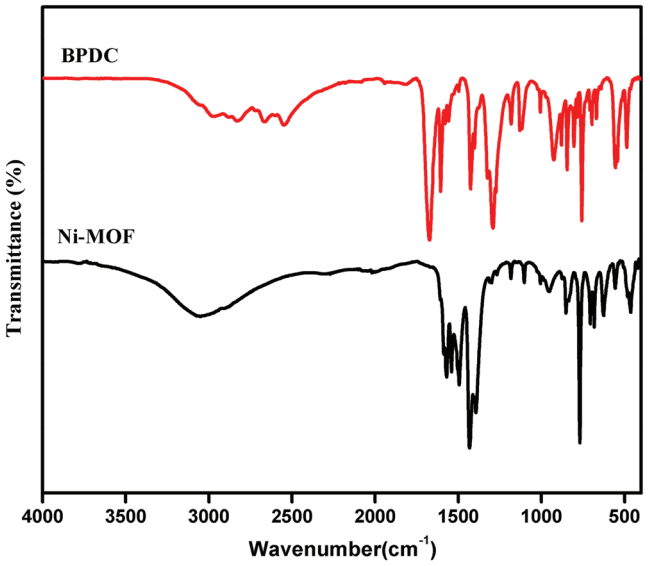

FIGURE 2 Fourier transform infrared spectra of nickel-based metal–organic framework (Ni-MOF) and 4,4′-biphenyldicarboxylic acid (BPDC)

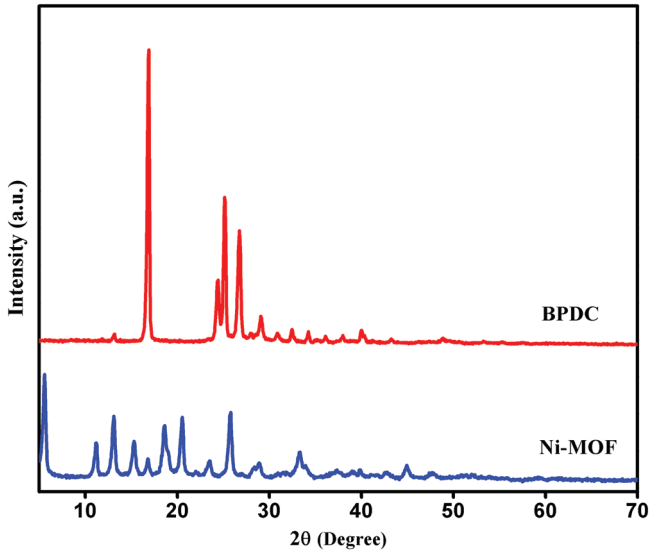

FIGURE 1 X-ray diffraction of nickel-based metal–organic framework (Ni-MOF) and 4,4′-biphenyldicarboxylic acid (BPDC)

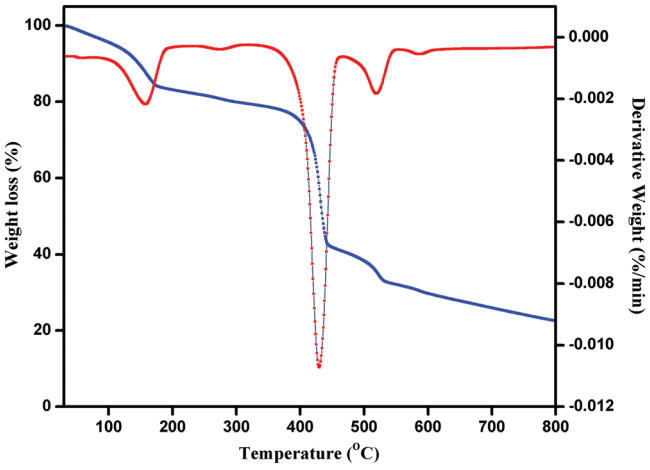

FIGURE 3 Thermogravimetry/differential thermal analysis spectra of nickel-based metal–organic framework

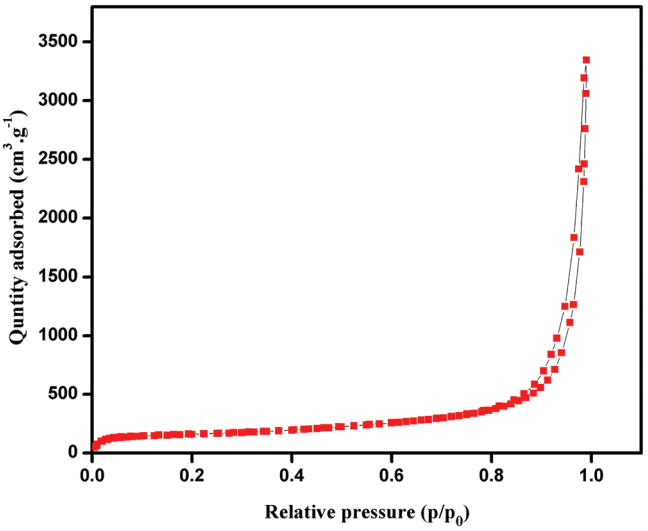

FIGURE 4 Nitrogen adsorption–desorption isotherms of nickel-based metal–organic framework

shows the nitrogen adsorption–desorption isotherm of Ni-MOF. Ni-MOF presents a type IV isotherm which is characteristic of mesoporous materials.[39] The BET surface area was found to be 353 m^2 g^{-1} and the total pore volume of Ni-MOF was 2.902 cm^3 g^{-1}. This high surface area and large pore dimensions of Ni-MOF can improve its catalytic performance.

We next performed a morphology study to understand the shape and size of synthesized Ni-MOF. A nanoplatelet-like morphology was noted , which is shown in Figure 5a. According to BET analysis results, Ni-MOF has an average diameter of 40–50 nm and larger pore dimensions. The energy-dispersive X-ray spectrum of Ni-MOF is depicted in Figure 5b, which shows the presence of only Ni, C, and O, thus confirming that Ni-MOF is free from impurities.

3.2 | Catalytic performance of Ni-MOF for the synthesis of α-aminophosphonates

Initially, the catalytic activity was evaluated with the coupling reaction of benzaldehyde, 3-(trifluoromethyl)aniline, and diethyl phosphite as a model reaction under a solvent-free condition to afford α-aminophosphonate. The performance of Ni-MOF as a catalyst in organic reactions mainly depends on the availability of catalytic sites, which is then governed by the choice of organic linkers and solvent/substrate polarity. Different solvents such as water, ethanol, acetonitrile, dichloromethane, and toluene were screened for the synthesis of α-aminophosphonate and their comparison with the solvent-free condition is presented in Table 1 (Entries 1–6). The solvent-free condition gave excellent yield (95%) compared with other solvents (Table 1, Entry 6). In the absence of catalyst, the yield of the desired product was only 39%, which proved that the presence of catalyst was necessary for the reaction to complete (Table 1, Entry 7). The effect of catalyst loading on reaction rate was evaluated by varying the amount of catalyst from 5, 10, 20, and 30 mg while keeping other parameters constant (Table 1, Entries 8–10). Hence, 10 mg of catalyst was enough to afford 95% of α-aminophosphonate (Table 1, Entry 6). Furthermore, the reaction was analyzed at different periods (Table 1, Entries 11–13), with the reaction quenched after 10 min, resulting in 75% yield which increased to 96% in 40 min.

To highlight the advantages of the Ni-MOF catalyst, the catalytic activity of the Ni-MOF was compared with other Ni-based MOFs including Ni-BDC Ni-BTC, and Ni-NDC and salts such as $NiCl_2$, $Ni(NO_3)_2$, and $Ni(OAc)_2$ (Table 2). Interestingly, it was observed that Ni-MOF with the organic ligand BPDC could achieve 95% conversion after 30 min due to high surface area and large pore

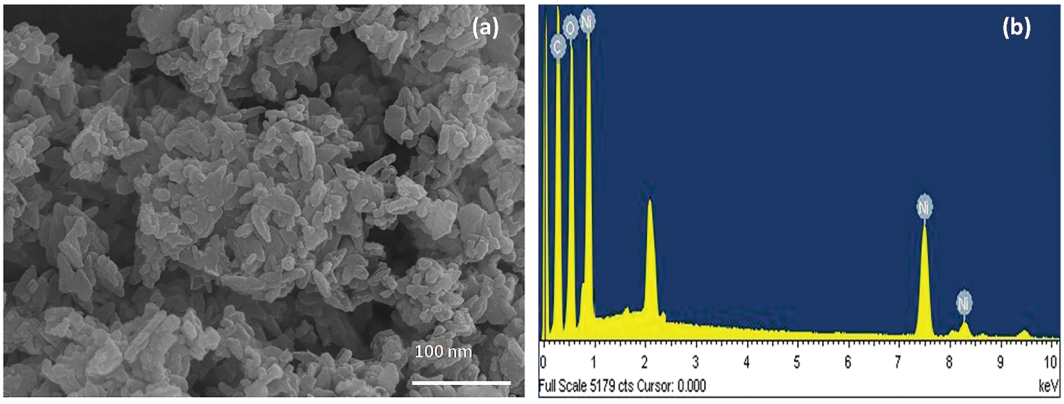

FIGURE 5 (a) Field-emission scanning electron microscopy and (b) energy-dispersive X-ray of nickel-based metal–organic framework

TABLE 1 Effect of parameter on synthesis of α-aminophosphonate[a]

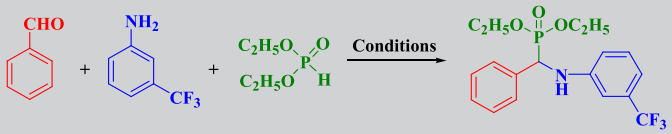

Entry	Catalyst amount (mg)	Solvent	Time (min)	Yield (%)[b]
1	10	Water	30	70
2	10	Ethanol	30	86
3	10	Acetonitrile	30	81
4	10	Dichloromethane	30	73
5	10	Toluene	30	52
6	10	Solvent free	30	95
7	–	Solvent free	30	39
8	5	Solvent free	30	89
9	20	Solvent free	30	95
10	30	Solvent free	30	96
11	10	Solvent free	10	75
12	10	Solvent free	20	81
13	10	Solvent free	40	96

[a]Reaction conditions: Benzaldehyde (1 mmol), 3-(trifluoromethyl)aniline (1 mmol), diethyl phosphite (1.2 mmol), nickel-based metal–organic framework (catalyst), and solvent (3 mL) at room temperature.
[b]Isolated yield.

TABLE 2 A comparison of the efficiency of nickel-based metal–organic framework (Ni-MOF) with other catalysts[a]

Entry	Catalyst	Catalyst amount (mg)	Time (min)	Yield (%)[b]
1	$NiCl_2$	20	30	34
2	$Ni(NO_3)_2$	20	30	31
3	$Ni(OAc)_2$	20	30	47
4[c]	Ni-BDC	10	30	71
5[d]	Ni-BTC	10	30	75
6[e]	Ni-NDC	10	30	88
7	Ni-MOF	10	30	95

[a]Reaction conditions: Benzaldehyde (1 mmol), 3-(trifluoromethyl)aniline (1 mmol), diethyl phosphite (1.2 mmol), and catalyst at room temperature.
[b]Isolated yield.
[c,d,e]Synthesized according to Sel and co-workers.[32]

dimensions of Ni-MOF, which provide more catalytic active sites that are responsible for catalysis (Table 2, Entry 7). Moreover, Ni-BDC Ni-BTC, and Ni-NDC yielded 71%, 75%, and 88% of the product (Table 2, Entries 4–6). However, it was observed that the reaction using $NiCl_2$, $Ni(NO_3)_2$, and $Ni(OAc)_2$ as catalyst gave only 31%–47% yield of the final product (Table 2, Entries 1–3). These observations would emphasize the advantages of using the Ni-MOF catalyst.

Different derivatives of α-aminophosphonate could be synthesized using the optimized reaction conditions (Table 3). A wide range of electron-withdrawing or electron-donating substituted aldehydes, including –Br, –Cl, –F, –OH, $-OCH_3$, and $-NO_2$ groups, were compatible with the optimized condition. All the electron-withdrawing or electron-donating substrates underwent reaction smoothly to afford the desired products in 80%–98% yields. In case of 2-thiophenecarboxaldehyde and ferrocene carbaldehyde, an excellent product was obtained in short period (Table 3, Entries 22 and 23). The synthesized α-aminophosphonate compounds were characterized by IR, ^{1}H NMR, ^{13}C NMR spectra, GC–MS, and elemental analysis (Supporting information).

4a. (Phenyl-[3-trifluoromethyl-phenylamino]-methyl)-phosphonic acid diethyl ester Yield 95% (white solid); melting point (MP) = 104–107 °C. IR (KBr, υ_{max}/cm^{-1}): 3294 (N–H), 1229 (P=O), 1054, 1013 (P–O–C), ^{1}H NMR (300 MHz, $CDCl_3$) δ = 7.47 (d, 2H, Ar), 7.39–7.22 (m, 3H, Ar), 7.17 (t, 1H, Ar), 7.06–6.60 (m, 3H, Ar), 5.27–5.06 (t, 1H, –NH), 4.76 (dd, 1H, –CH), 4.24–3.56

TABLE 3 Scope of different aldehydes for the synthesis of α-aminophosphonates[a]

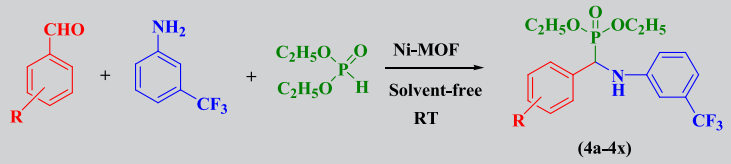

Entry	R	Product	Time (min)	Yield (%)[b]
1	Benzaldehyde	**4a**	30	95[c]
2	2-Methoxybenzaldehyde	**4b**	30	94
3	3-Methoxybenzaldehyde	**4c**	45	98
4	4-Methoxybenzaldehyde	**4d**	45	93[c]
5	3,4-Dimethoxybenzaldehyde	**4e**	45	95
6	2,5-Dimethoxybenzaldehyde	**4f**	30	96
7	3,4,5-Trimethoxybenzaldehyde	**4g**	30	98
8	2-Hydroxy-3-methoxybenzaldehyde	**4h**	45	96
9	3-Hydroxybenzaldehyde	**4i**	60	95
10	4-Hydroxybenzaldehyde	**4j**	60	96
11	4-Chlorobenzaldehyde	**4k**	45	95
12	4-Bromobenzaldehyde	**4l**	45	95
13	2-Fluorobenzaldehyde	**4m**	45	92
14	3-Fluorobenzaldehyde	**4n**	45	91
15	4-Fluorobenzaldehyde	**4o**	60	94
16	3,4-Difluorobenzaldehyde	**4p**	45	90
17	4-(Trifluoromethyl)benzaldehyde	**4q**	60	90
18	2-Nitrobenzaldehyde	**4r**	60	90
119	3-Nitrobenzaldehyde	**4s**	60	92
20	4-(Dimethylamino)benzaldehyde	**4t**	45	90
21	4-(Benzyloxy)benzaldehyde	**4u**	60	96
22	Ferrocene carbaldehyde	**4v**	60	97
23	2-Thiophenecarboxaldehyde	**4w**	45	94
24	3,5-Dimethylbenzaldehyde	**4x**	45	90

[a]Reaction condition: Aldehydes (1 mmol), 3-(trifluoromethyl)aniline (1 mmol), diethyl phosphite (1.2 mmol), nickel-based metal–organic framework (10 mg), and solvent-free condition at room temperature.
[b]Isolated yield.
[c]Reported compound.

(m, 4H, $-OCH_2CH_3$), 1.29 (t, 3H, $-OCH_2CH_3$), 1.10 (t, 3H, $-OCH_2CH_3$). ^{13}C NMR (75 MHz, $CDCl_3$) δ = 146.83 (d, J = 14.6 Hz), 135.39 (d, J = 2.6 Hz), 131.40 (d, J = 31.8 Hz), 129.58, 128.72 (d, J = 2.6 Hz), 128.05 (dd, J = 18.0, 4.4 Hz), 124.22 (d, J = 272.3 Hz), 116.31 (s), 114.58 (q, J = 3.8 Hz), 110.60 (q, J = 3.9 Hz), 63.51 (d, J = 7.0 Hz, $-OCH_2CH_3$), 63.27 (d, J = 7.1 Hz, $-OCH_2CH_3$), 56.87–54.86 (J = 151.7 Hz, –CH), 16.42 (d, J = 5.8 Hz, $-OCH_2CH_3$), 16.16 (d, J = 5.8 Hz, $-OCH_2CH_3$). Anal. calcd. for $C_{18}H_{21}F_3NO_3P$: C, 55.82; H, 5.46; N, 3.62; found: C, 55.71; H, 5.35; N, 3.54.

4b. ([2-Methoxy-phenyl]-[3-trifluoromethyl-phenylamino]-methyl)-phosphonic acid diethyl ester Yield 94% (white solid); MP = 143–146 °C. IR (KBr, υ_{max}/cm^{-1}): 3276 (N–H), 1228 (P=O), 1043, 1019 (P–O–C), ^1H NMR (300 MHz, $CDCl_3$) δ = 7.48 (d, 1H, Ar), 7.34–6.84 (m, 6H, Ar), 6.74 (d, 1H, Ar), 5.39 (dd, 1H, –CH), 5.09 (t, 1H, –NH), 4.33–4.07 (m, 2H, $-OCH_2CH_3$),

4.08–3.39 (m, 5H, $-OCH_3$ and $-OCH_2CH_3$), 1.32 (t, 3H, $-OCH_2CH_3$), 1.03 (t, 3H, $-OCH_2CH_3$). ^{13}C NMR (75 MHz, $CDCl_3$) δ = 157.27 (d, J = 6.6 Hz), 146.78 (d, J = 14.8 Hz), 131.39 (d, J = 31.7 Hz), 126.11, 123.99, 122.51, 121.13 (d, J = 2.8 Hz), 116.68, 114.47 (d, J = 2.8 Hz), 110.52 (d, J = 1.9 Hz), 109.85 (d, J = 4.0 Hz), 63.36 (d, J = 7.1 Hz, $-OCH_2CH_3$), 63.07 (d, J = 6.9 Hz, $-OCH_2CH_3$), 55.73 ($-OCH_3$), 48.55–46.49 (J = 155.8 Hz, –CH), 16.44 (d, J = 5.9 Hz, $-OCH_2CH_3$), 16.09 (d, J = 5.9 Hz, $-OCH_2CH_3$). Anal. calcd. for $C_{19}H_{23}F_3NO_4P$: C, 54.68; H, 5.55; N, 3.36; found: C, 54.68; H, 5.35; N, 3.06. GC–MS (electron ionization [EI]) *m/z* (%) calcd.: 417; found: 417, 280.

4d. ([4-Methoxy-phenyl]-[3-trifluoromethyl-phenylamino]-methyl)-phosphonic acid diethyl ester Yield 93% (white solid); MP = 111–113 °C. IR (KBr, υ_{max}/cm^{-1}): 3306 (N–H), 1229 (P=O), 10459, 1038 (P–O–C), ^1H NMR (300 MHz, $CDCl_3$) δ = 7.51–7.33 (m, 2H, Ar), 7.17 (t, 1H, Ar), 6.96–6.83 (m, 4H, Ar), 6.71 (d, 1H, Ar), 5.14 (t, 1H, –NH), 4.71 (dd, 1H, –CH), 4.12 (m, 2H, $-OCH_2CH_3$), 4.00–3.64 (m, 5H, $-OCH_2CH_3$ and $-OCH_3$), 1.21 (tt, 6H, $-OCH_2CH_3$). ^{13}C NMR (75 MHz, $CDCl_3$) δ = 159.49 (d, J = 2.8 Hz), 146.69 (d, J = 14.6 Hz), 131.42 (q, J = 31.8 Hz), 129.59, 128.98 (d, J = 5.6 Hz), 127.01 (d, J = 2.6 Hz), 125.98, 122.37, 116.52, 114.70 (d, J = 3.9 Hz), 114.19 (d, J = 1.8 Hz), 110.44 (d, J = 3.8 Hz), 63.46 (J = 7.0 Hz, $-OCH_2CH_3$), 63.20 (J = 7.1 Hz, $-OCH_2CH_3$), 56.21 ($-OCH_3$), 55.24–54.18 (J = 80.5 Hz, –CH), 16.44 (J = 5.8 Hz, $-OCH_2CH_3$), 16.26 (J = 5.7 Hz, $-OCH_2CH_3$). Anal. calcd. for $C_{19}H_{23}F_3NO_4P$: C, 54.68; H, 5.55; N, 3.36; found: C, 53.61; H, 5.35; N, 3.06.

4e. ([3,4-Dimethoxy-phenyl]-[3-trifluoromethyl-phenylamino]-methyl)-phosphonic acid diethyl ester Yield 95% (white solid); MP = 90–93 °C. IR (KBr, υ_{max}/cm^{-1}): 3301 (N–H), 1230 (P=O), 1056, 1030 (P–O–C), ^1H NMR (300 MHz, $CDCl_3$) δ= 7.19 (t, 1H, Ar), 6.93 (m, 5H, Ar), 6.72 (d, 1H, Ar), 5.01 (s, 1H, –NH), 4.70 (d, 1H, –CH), 4.21–3.60 (m, 10H, $-OCH_3$ and $-OCH_2CH_3$), 1.30 (t, 3H, $-OCH_2CH_3$), 1.14 (t, 3H, $-OCH_2CH_3$). ^{13}C NMR (75 MHz, $CDCl_3$) δ = 149.11 (dd, J = 21.5, 2.8 Hz), 146.84 (d, J = 14.5 Hz), 131.44 (q, J = 31.8 Hz), 129.61, 127.60 (d, J = 2.7 Hz), 126.02, 122.41, 120.32 (d, J = 6.4 Hz), 116.58, 114.78, 111.24 (d, J = 2.4 Hz), 110.92 (d, J = 4.9 Hz), 110.63–110.25, 63.50 (J = 7.0 Hz, $-OCH_2CH_3$), 63.23 (J = 7.1 Hz, $-OCH_2CH_3$), 56.65 ($-OCH_3$), 55.98 ($-OCH_3$), 55.87–54.62 (–CH), 16.45 (J = 5.8 Hz, $-OCH_2CH_3$), 16.30 (J = 5.7 Hz, $-OCH_2CH_3$). Anal. calcd. for $C_{20}H_{25}F_3NO_5P$: C, 53.69; H, 5.63; N, 3.13; found: C, 53.56; H, 5.39; N, 3.03. GC–MS (EI) *m/z* (%) calcd.: 447; found: 447, 310.

4f. ([2,5-Dimethoxy-phenyl]-[3-trifluoromethyl-phenylamino]-methyl)-phosphonic acid diethyl ester Yield 96% (white solid); MP = 127–130 °C. IR (KBr, υ_{max}/cm^{-1}): 3310 (N–H), 1230 (P=O), 1056, 1021 (P–O–C), ^1H NMR (300 MHz, $CDCl_3$) δ = 7.23–7.01 (m, 2H, Ar), 6.98–6.67 (m, 5H, Ar), 5.37 (dd, 1H, –CH), 5.16 (t, 1H, –NH), 4.19 (m, 2H, $-OCH_2CH_3$), 4.04–3.81 (m, 4H, $-OCH_3$ and $-OCH_2CH_3$), 3.81–3.55 (m, 4H, $-OCH_2CH_3$ and $-OCH_3$), 1.32 (t, 3H, $-OCH_2CH_3$), 1.07 (t, 3H, $-OCH_2CH_3$). ^{13}C NMR (75 MHz, $CDCl_3$) δ = 153.98 (d, J = 3.0 Hz), 151.57 (d, J = 6.6 Hz), 146.75 (d, J = 14.8 Hz), 131.42 (q, J = 31.7 Hz), 129.51, 125.05, 116.73, 114.57 (q, J = 3.9 Hz), 114.11 (dd, J = 6.2, 3.8 Hz), 111.66 (d, J = 2.0 Hz), 109.85 (q, J = 4.0 Hz), 63.39 (J = 7.0 Hz, $-OCH_2CH_3$), 63.11 (J = 6.9 Hz, $-OCH_2CH_3$), 56.27 ($-OCH_3$), 55.66–47.74 (J = 155.3 Hz, –CH), 16.44 (J = 5.8 Hz, $-OCH_2CH_3$), 16.14 (J = 5.9 Hz, $-OCH_2CH_3$). Anal. calcd. for $C_{20}H_{25}F_3NO_5P$: C, 53.69; H, 5.63; N, 3.13; found: C, 53.60; H, 5.43; N, 3.01.

4g. ([3-Trifluoromethyl-phenylamino]-[3,4,5-trimethoxy-phenyl]-methyl)-phosphonic acid diethyl ester Yield 98% (white solid); MP = 117–119 °C. IR (KBr, υ_{max}/cm^{-1}): 3301 (N–H), 1231 (P=O), 1030, 1012 (P–O–C), ^1H NMR (300 MHz, $CDCl_3$) δ = 7.22 (t, 1H, Ar), 7.03–6.86 (m, 2H, Ar), 6.72 (m, 3H, Ar), 5.17–4.94 (t, 1H, –NH), 4.67 (dd, 1H, –CH), 4.13 (m, 2H, $-OCH_2CH_3$), 4.06–3.79 (m, 10H, $-OCH_2CH_3$ and $-OCH_3$), 3.72 (m, 1H, $-OCH_2CH_3$), 1.30 (t, 3H, $-OCH_2CH_3$), 1.15 (t, 3H, $-OCH_2CH_3$). ^{13}C NMR (75 MHz, $CDCl_3$) δ = 153.50 (d, J = 2.7 Hz), 146.83 (d, J = 14.3 Hz), 137.88 (d, J = 3.6 Hz), 132.39–130.63, 129.69, 126.01, 122.40, 116.55, 114.90, 111.24–109.22, 104.94, 63.53 (d, J = 7.0 Hz, $-OCH_2CH_3$), 63.29 (d, J = 7.1 Hz, $-OCH_2CH_3$), 60.86 (d, $-OCH_3$), 57.21 ($-OCH_3$), 56.19–55.19 (–CH), 16.46 (d, J = 5.8 Hz, $-OCH_2CH_3$), 16.29 (d, J = 5.8 Hz, $-OCH_2CH_3$). Anal. calcd. for $C_{21}H_{27}F_3NO_6P$: C, 52.83; H, 5.70; N, 2.93; found: C, 52.51; H, 5.49; N, 2.75.

4h. ([2-Hydroxy-3-methoxy-phenyl]-[3-trifluoromethyl-phenylamino]-methyl)-phosphonic acid diethyl ester Yield 96% (white solid); MP = 148–150 °C. IR (KBr, υ_{max}/cm^{-1}): 3465 (N–H), 1229 (P=O), 1058, 1011 (P–O–C), ^1H NMR (300 MHz, $CDCl_3$) δ = 6.97 (m, 7H, Ar), 6.41 (s, 1H, Ar), 5.26 (dd, 1H, –CH), 5.06 (t, 1H, –NH), 4.28–4.07 (m, 2H, $-OCH_2CH_3$), 4.06–3.58 (m, 5H, $-OCH_3$ and $-OCH_2CH_3$), 1.31 (t, 3H, $-OCH_2CH_3$), 1.10 (t, 3H, $-OCH_2CH_3$). ^{13}C NMR (75 MHz, $CDCl_3$) δ = 146.81 (dd, J = 13.4, 8.0 Hz), 144.01 (d, J = 6.6 Hz), 131.45 (q, J = 31.8 Hz), 129.60, 125.11, 122.47, 121.62, 120.37, 118.91, 116.49, 115.00–113.77, 110.50, 110.33, 63.50 (J = 7.1 Hz, $-OCH_2CH_3$), 63.34 (J = 7.0 Hz, $-OCH_2CH_3$), 56.09 ($-OCH_3$), 50.03–47.97 (J = 155.8 Hz, –CH), 16.42 (d, J = 5.8 Hz, $-OCH_2CH_3$), 16.14 (d, J = 5.7 Hz, $-OCH_2CH_3$). Anal. calcd. for $C_{19}H_{23}F_3NO_5P$: C, 52.66; H, 5.35; N, 3.23; found: C, 52.56; H, 5.23; N, 3.02. GC–MS (EI) *m/z* (%) calcd.: 433; found: 433, 295.

4i. ([3-Hydroxy-phenyl]-[3-trifluoromethyl-phenylamino]-methyl)-phosphonic acid diethyl ester Yield 95% (white solid); MP = 149–152 °C. IR (KBr, υ_{max}/cm^{-1}): 3310 (N–H), 1231 (P=O), 1049, 1018 (P–O–C), ^{1}H NMR (300 MHz, $CDCl_3$) δ = 7.27–7.05 (m, 3H, Ar), 7.00–6.74 (m, 4H, Ar), 6.66 (d, 1H, Ar), 5.08 (s, 1H, –NH), 4.71 (d, 1H, –CH), 4.23–3.80 (m, 3H, $-OCH_2CH_3$), 3.58 (m, 1H, $-OCH_2CH_3$), 1.28 (t, 3H, $-OCH_2CH_3$), 1.04 (t, 3H, $-OCH_2CH_3$). ^{13}C NMR (75 MHz, $CDCl_3$) δ = 157.41 (d, *J* = 3.0 Hz), 146.48 (d, *J* = 14.3 Hz), 136.34 (d, *J* = 2.4 Hz), 131.44, 129.98, 124.13, 120.04, 116.37, 116.06, 114.86, 114.14, 110.44, 64.22 (d, *J* = 7.2 Hz, $-OCH_2CH_3$), 63.68 (d, *J* = 7.3 Hz, $-OCH_2CH_3$), 55.71 (*J* = 152.9 Hz, –CH), 16.32 (d, *J* = 5.8 Hz, $-OCH_2CH_3$), 16.05 (d, *J* = 5.7 Hz, $-OCH_2CH_3$). Anal. calcd. for $C_{18}H_{21}F_3NO_4P$: C, 53.60; H, 5.25; N, 3.47;

4j. ([4-Hydroxy-phenyl]-[3-trifluoromethyl-phenylamino]-methyl)-phosphonic acid diethyl ester Yield 96% (white solid); MP = 96–98 °C. IR (KBr, υ_{max}/cm^{-1}): 3361 (N–H), 1229 (P=O), 1058, 1018 (P–O–C), ^{1}H NMR (300 MHz, $CDCl_3$) δ = 7.57–7.32 (m, 2H, Ar), 7.26–6.78 (m, 5H, Ar), 6.69 (d, 1H, Ar), 5.36–5.02 (t, 1H, –NH), 4.75 (dd, 1H, –CH), 4.29–3.87 (m, 3H, $-OCH_2CH_3$), 3.84–3.64 (m, 1H, $-OCH_2CH_3$), 1.22 (m, 6H, $-OCH_2CH_3$). ^{13}C NMR (75 MHz, $CDCl_3$) δ = 156.87 (d, *J* = 2.7 Hz), 146.56 (d, *J* = 14.3 Hz), 131.45 (q, *J* = 32.0 Hz), 129.63, 125.33, 122.37, 116.71, 116.08, 114.90, 110.48, 63.80 (d, *J* = 6.8 Hz, $-OCH_2CH_3$), 63.71 (d, *J* = 7.1 Hz, $-OCH_2CH_3$), 56.13–54.08 (*J* = 154.7 Hz, –CH), 16.34 (d, *J* = 5.6 Hz, $-OCH_2CH_3$), 16.16 (d, *J* = 5.7 Hz, $-OCH_2CH_3$). Anal. calcd. for $C_{18}H_{21}F_3NO_4P$: C, 53.60; H, 5.25; N, 3.47; found: C, 53.10; H, 5.01; N, 3.13.

4l. ([4-Bromo-phenyl]-[3-trifluoromethyl-phenylamino]-methyl)-phosphonic acid diethyl ester Yield 95% (white solid); MP = 99–101 °C. IR (KBr, υ_{max}/cm^{-1}): 3298 (N–H), 1231 (P=O), 1053, 1021 (P–O–C), ^{1}H NMR (300 MHz, $CDCl_3$) δ = 7.52–7.34 (dd, 4H, Ar), 7.18 (t, 1H, Ar), 7.03–6.81 (m, 2H, Ar), 6.67 (d, 1H, Ar), 5.51–5.30 (t, 1H, –NH), 4.73 (dd, 1H, –CH), 4.24–3.94 (m, 3H, $-OCH_2CH_3$), 3.86–3.67 (m, 1H, $-OCH_2CH_3$), 1.23 (m, 6H, $-OCH_2CH_3$). ^{13}C NMR (75 MHz, $CDCl_3$) δ = 146.47 (d, *J* = 14.5 Hz), 134.03 (d, *J* = 3.0 Hz), 131.75 (t, *J* = 31.9 Hz), 129.64, 129.17, 128.94, 125.93, 122.32, 116.36, 114.95, 110.53, 64.10–62.68, 56.35–54.34 (*J* = 151.6 Hz, –CH), 16.41 (*J* = 5.7 Hz, $-OCH_2CH_3$), 16.22 (*J* = 5.7 Hz, $-OCH_2CH_3$). Anal. calcd. for $C_{18}H_{20}BrF_3NO_3P$: C, 46.37; H, 4.32; N, 3.00; found: C, 46.07; H, 4.00; N, 2.96. GC–MS (EI) *m/z* (%) calcd.: 466; found: 465, 328, 172, 145.

4o. ([4-Fluoro-phenyl]-[3-trifluoromethyl-phenylamino]-methyl)-phosphonic acid diethyl ester Yield 94% (white solid); MP = 106–108 °C. IR (KBr, υ_{max}/cm^{-1}): 3297 (N–H), 1224 (P=O), 1048, 1017 (P–O–C), 1H NMR (300 MHz, $CDCl_3$) δ = 7.26–7.15(m, 3H, Ar), 6.93–6.86 (m, 2H, Ar), 6.73–4.67 (dd, 3H, Ar), 4.15–4.10 (d, 1H, –CH), 4.07–3.92 (m, 3H, $-OCH_2CH_3$), 3.78–3.73 (m, 1H, $-OCH_2CH_3$), 1.29–1.25(t, 3H, $-OCH_2CH_3$), 1.16–1.11 (t, 3H, $-OCH_2CH_3$). ^{13}C NMR (75 MHz, $CDCl_3$) δ = 162.58 (dd, *J* = 247.0, 3.4 Hz), 146.57 (d, *J* = 14.6 Hz), 132.48–130.74, 129.72–129.36, 125.96, 122.35, 116.41, 115.74, 115.16–114.48, 110.52, 63.51 (d, *J* = 7.2 Hz, $-OCH_2CH_3$), 63.40 (d, *J* = 7.2 Hz, $-OCH_2CH_3$), 56.21–54.19 (*J* = 152.5 Hz, –CH), 16.43 (d, *J* = 5.7 Hz, $-OCH_2CH_3$), 16.22 (d, *J* = 5.7 Hz, $-OCH_2CH_3$). Anal. calcd. for $C_{18}H_{20}F_4NO_3P$: C, 53.34; H, 4.97; N, 3.46: found: C, 53.01; H, 4.80; N, 3.12. GC–MS (EI) *m/z* (%) calcd.: 405; found: 405, 267, 172, 145.

4q. ([4-Trifluoromethyl-phenyl]-[3-trifluoromethyl-phenylamino]-methyl)-phosphonic acid diethyl ester Yield 90% (white solid); MP = 103–105 °C. IR (KBr, υ_{max}/cm^{-1}): 3280 (N–H), 1228 (P=O), 1048, 1015 (P–O–C), ^{1}H NMR (300 MHz, $CDCl_3$) δ = 7.61 (s, 4H, Ar), 7.19 (t, 1H, Ar), 6.95 (d, 1H, Ar), 6.85 (s, 1H, Ar), 6.66 (d, 1H, Ar), 5.31–5.14 (t, 1H, –NH), 4.83 (dd, 1H, –CH), 4.24–3.72 (m, 4H, $-OCH_2CH_3$), 1.31 (t, 3H, $-OCH_2CH_3$), 1.16 (t, 3H, $-OCH_2CH_3$). ^{13}C NMR (75 MHz, $CDCl_3$) δ = 146.48 (d, *J* = 14.4 Hz), 139.90, 132.02 (d, *J* = 31.9 Hz), 130.41, 129.77, 128.25, 125.95, 125.70, 122.27, 116.17, 115.04, 110.68, 63.68 (d, *J* = 7.2 Hz, $-OCH_2CH_3$), 63.58 (d, *J* = 7.2 Hz, $-OCH_2CH_3$), 56.68–54.68 (*J* = 150.8 Hz, –CH), 16.44 (d, *J* = 5.7 Hz, $-OCH_2CH_3$), 16.19 (d, *J* = 5.7 Hz, $-OCH_2CH_3$). Anal. calcd. for $C_{19}H_{20}F_6NO_3P$: C, 50.12; H, 4.43; N, 3.08; found: C, 50.00; H, 4.13; N, 2.98.

4r. ([2-Nitro-phenyl]-[3-trifluoromethyl-phenylamino]-methyl)-phosphonic acid diethyl ester Yield 90% (buff solid); MP = 145–147 °C. IR (KBr, υ_{max}/cm^{-1}): 3301 (N–H), 1231 (P=O), 1042, 1011 (P–O–C), ^{1}H NMR (300 MHz, $CDCl_3$) δ = 8.02 (d, 1H, Ar), 7.76 (d, 1H, Ar), 7.50 (m, 2H, Ar), 7.22 (t, 1H, Ar), 7.09–6.88 (m, 2H, Ar), 6.81 (d, 1H, Ar), 6.18 (dd, 1H, –CH), 5.62 (t, 1H, –NH), 4.19 (m, 2H, $-OCH_2CH_3$), 4.05–3.63 (m, 2H, $-OCH_2CH_3$), 1.32 (t, 3H, $-OCH_2CH_3$), 1.11 (t, 3H, $-OCH_2CH_3$). ^{13}C NMR (75 MHz, $CDCl_3$) δ = 149.55 (d, *J* = 5.5 Hz), 146.16 (d, *J* = 14.5 Hz), 133.51 (d, *J* = 3.0 Hz), 131.71, 131.16, 129.93, 128.86, 125.93, 125.28, 122.32, 115.67, 115.01, 110.89, 64.01 (d, *J* = 7.2 Hz, $-OCH_2CH_3$), 63.52 (d, *J* = 7.2 Hz, $-OCH_2CH_3$), 50.73–48.71 (*J* = 150.8 Hz, –CH), 16.38 (d, *J* = 5.7 Hz, $-OCH_2CH_3$), 15.94 (d, *J* = 5.7 Hz, $-OCH_2CH_3$). Anal. calcd. for $C_{18}H_{20}F_3N_2O_5P$: C, 50.01; H, 4.66; N, 6.48; found: C, 49.97; H, 4.60; N, 6.39. GC–MS (EI) *m/z* (%) calcd.: 432; found: 432, 295, 145.

4s. ([3-Nitro-phenyl]-[3-trifluoromethyl-phenylamino]-methyl)-phosphonic acid diethyl ester Yield 92% (yellow solid); MP = 116–118 °C. IR (KBr, υ_{max}/cm^{-1}): 3295 (N–H), 1236 (P=O), 1046, 1019 (P–O–C), ^{1}H NMR (300 MHz, $CDCl_3$) δ = 8.36 (s, 1H, Ar), 8.17

(d, 1H, Ar), 7.84 (d, 1H, Ar), 7.54 (t, 1H, Ar), 7.21 (t, 1H, Ar), 6.97 (d, 1H, Ar), 6.85 (s, 1H, Ar), 6.68 (d, 1H, –CH), 5.47–5.23 (t, 1H, –NH), 4.92–4.88 (dd, 1H, $-OCH_2CH_3$), 4.31–3.79 (m, 4H, $-OCH_2CH_3$), 1.32 (t, 3H, $-OCH_2CH_3$), 1.19 (t, 3H, $-OCH_2CH_3$). ^{13}C NMR (75 MHz, $CDCl_3$) δ = 148.53 (d, J = 3.0 Hz), 146.28 (d, J = 14.2 Hz), 138.33 (d, J = 2.5 Hz), 133.86 (d, J = 5.0 Hz), 131.60 (q, J = 31.9 Hz), 129.82, 129.66, 125.88, 123.16, 122.76, 116.10, 115.22, 110.69, 63.89 (d, J = 7.1 Hz, $-OCH_2CH_3$), 63.63 (d, J = 7.1 Hz, $-OCH_2CH_3$), 56.39–54.38 (J = 151.3 Hz, –CH), 16.43 (d, J = 5.7 Hz, $-OCH_2CH_3$), 16.22 (d, J = 5.7 Hz, $-OCH_2CH_3$). Anal. calcd. for $C_{18}H_{20}F_3N_2O_5P$: C, 50.01; H, 4.66; N, 6.48; found: C, 49.90; H, 4.60; N, 6.37.

4t. ([4-Dimethylamino-phenyl]-[3-trifluoromethyl-phenylamino]-methyl)-phosphonic acid diethyl ester Yield 90% (white solid); MP = 102–104 °C. IR (KBr, υ_{max}/cm^{-1}): 3279 (N–H), 1226 (P=O), 1058, 1016 (P–O–C), ^1H NMR (300 MHz, $CDCl_3$) δ = 7.31 (d, 2H, Ar), 7.16 (t, 1H, Ar), 6.89 (d, 2H, Ar), 6.70 1(t, 3H, Ar), 5.03 (t, 1H, –NH), 4.66 (dd, 1H, –CH), 4.12 (m, 1H, $-OCH_2CH_3$), 4.01–3.81 (m, 1H, $-OCH_2CH_3$), 3.65 (m, 1H, $-OCH_2CH_3$), 2.92 (s, 6H, $-CH_3$), 1.29 (t, 3H, $-OCH_2CH_3$), 1.13 (t, 3H, $-OCH_2CH_3$). ^{13}C NMR (75 MHz, $CDCl_3$) δ = 150.35 (d, J = 2.4 Hz), 146.96 (d, J = 14.6 Hz), 131.33 (q, J = 31.7 Hz), 129.52, 128.67, 124.26, 122.20, 116.50, 114.42, 112.54, 110.50, 63.39 (d, J = 7.0 Hz, $-OCH_2CH_3$), 63.03 (d, J = 7.0 Hz, $-OCH_2CH_3$), 56.21–54.17 (J = 154.2 Hz, –CH), 40.42 ($-CH_3$), 16.45 (d, J = 5.7 Hz, $-OCH_2CH_3$), 16.30 (d, J = 5.7 Hz, $-OCH_2CH_3$). Anal. calcd. for $C_{20}H_{26}F_3N_2O_3P$: C, 55.81; H, 6.09; N, 6.51; found: C, 55.70; H, 6.00; N, 6.36.

4w. (Thiophen-2-yl-[3-trifluoromethyl-phenylamino]-methyl)-phosphonic acid diethyl ester Yield 94% (white solid); MP = 96–99 °C. IR (KBr, υ_{max}/cm^{-1}): 3296 (N–H), 1227 (P=O), 1043, 1012 (P–O–C), ^1H NMR (300 MHz, $CDCl_3$) δ = 7.36–7.13 (m, 3H, Ar), 6.97 (dd, 3H), 6.81 (m, 1H, Ar), 5.27–4.91 (m, 2H, –CH and –NH), 4.28–3.74 (m, 4H, $-OCH_2CH_3$), 1.24 (m, 6H, $-OCH_2CH_3$). ^{13}C NMR (75 MHz, $CDCl_3$) δ = 146.55 (d, J = 13.1 Hz), 138.99 (d, J = 1.7 Hz), 131.50 (q, J = 31.9 Hz), 129.67, 127.19, 126.54, 125.54, 122.3, 116.59, 115.19, 110.56, 63.70 (d, J = 3.6 Hz, $-OCH_2CH_3$), 63.60 (d, J = 3.6 Hz, $-OCH_2CH_3$), 52.84–50.74 (J = 158.8 Hz, –CH), 16.42 (d, J = 5.8 Hz, $-OCH_2CH_3$), 16.26 (d, J = 5.8 Hz, $-OCH_2CH_3$). Anal. calcd. for $C_{16}H_{19}F_3NO_3PS$: C, 48.85; H, 4.87; N, 3.56; found: C, 48.59; H, 4.70; N, 3.46; S, 8.00. GC–MS (EI) m/z (%) calcd.: 393; found: 393, 256.

An excellent catalytic performance of Ni-MOF is due to its higher surface area and large pore dimensions. In metal carboxylates, the metal–oxygen bond (M^{n+}–O^{2-}), which acts as the Lewis acid site and basic site, respectively, is responsible for catalysis. The plausible mechanism for the synthesis of α-aminophosphonate over Ni-MOF is depicted in Figure 6. In the mechanism, the Lewis acid site of Ni-MOF activates the carbonyl group of aldehyde to form imine. The Lewis acid site of Ni-MOF further activates the imine and then the activated complex reacts with diethyl phosphite to afford α-aminophosphonate with regeneration of Ni-MOF for further reaction.

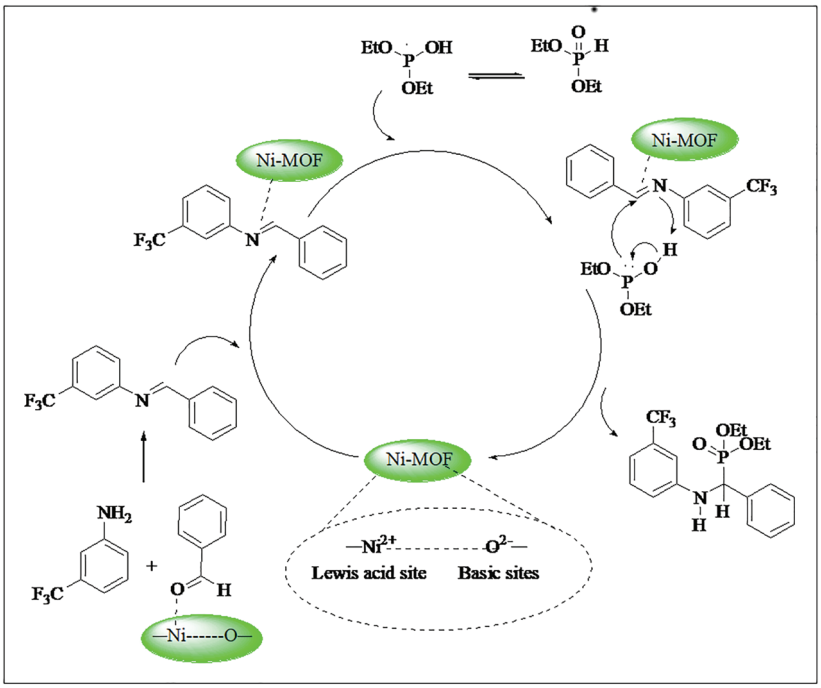

FIGURE 6 Plausible mechanism for α-aminophosphonate synthesis using nickel-based metal–organic framework (Ni-MOF)

FIGURE 7 Recyclability of catalyst

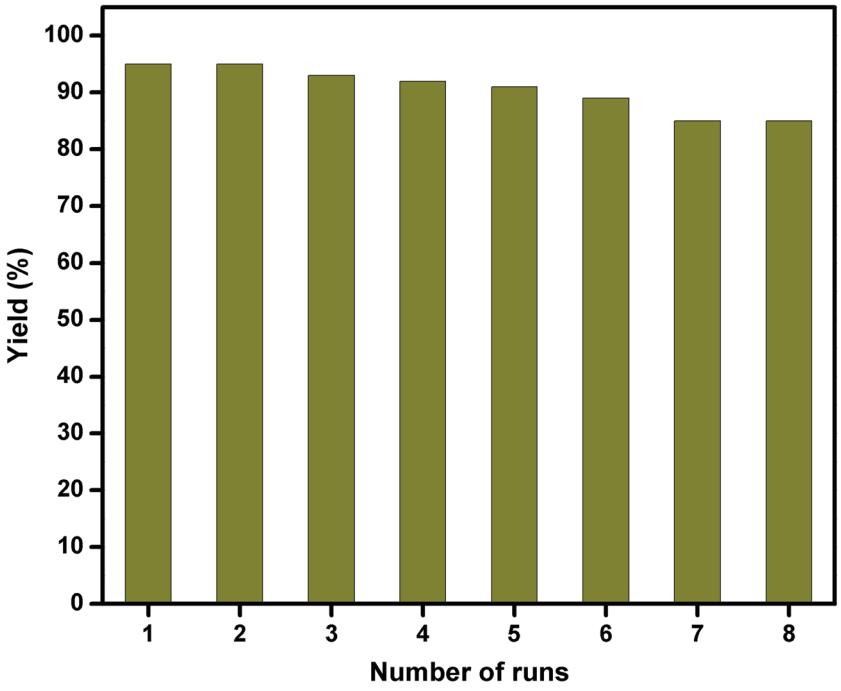

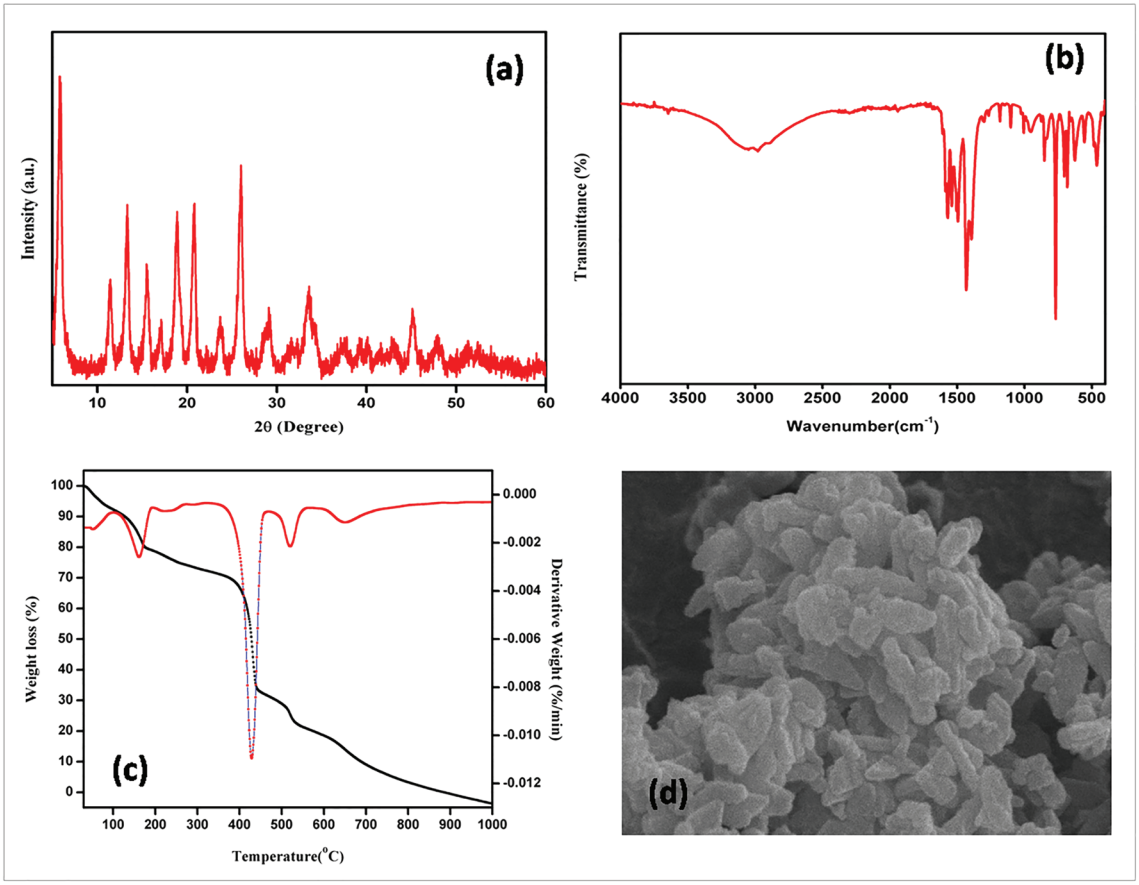

FIGURE 8 (a) X-ray diffraction, (b) Fourier transform infrared, (c) thermogravimetry/differential thermal analysis, and (d) field-emission scanning electron microscopy of nickel-based metal–organic framework (eighth run)

3.3 | Recycling of catalyst

The recyclability of the catalyst plays a vital role in industrial and chemical processes. Ni-MOF was employed as a recyclable catalyst in the formation of α-aminophosphonate via benzaldehyde and diethyl phosphite with 3-(trifluoromethyl)aniline under optimized reaction conditions. The catalyst was separated from the reaction mixture by centrifugation after each run and then washed with ethanol and dried overnight at 80 °C. Experimental results indicated that the Ni-MOF catalyst could be reused up to the eighth run. Indeed, the reaction still afforded 85% yield in the eighth run (Figure 7). Furthermore, the catalyst Ni-MOF could be maintained during the reaction as confirmed by XRD, FTIR, TG-DTA, BET, and FESEM results of the recovered Ni-MOF (Figure 8). The XRD of recycled Ni-MOF showed slightly different crystallinity than the fresh Ni-MOF. The FTIR spectra of recycled Ni-MOF exhibited a similar absorption as compared with that of fresh Ni-MOF. The catalyst recycled after the eighth run shows a slight decrease in the weight loss due to removal of physically adsorbed solvent and other organic impurities. FESEM and BET studies of the recycled catalyst show agglomerated nanoplatelets with decreases in pore size of Ni-MOF due to use of the catalyst in several reactions. The percentage of nickel present in fresh and reused Ni-MOF was analyzed by inductively coupled plasma atomic emission spectroscopy and was found to be invariable.

TABLE 4 Antibacterial and antioxidant activities of novel α-aminophosphonate derivatives

	Minimum inhibitory concentration (μg/mL)				2,2-Diphenyl-1-picrylhydrazyl radical scavenging activity
Compounds	*Staphylococcus aureus*	*Bacillus subtilis*	*Escherichia coli*	*Salmonella typhi*	Half-maximal inhibitory concentration (μg/mL)
4a	250	250	250	250	312.61
4b	125	15.62	31.25	62.5	105.85
4c	62.5	250	250	125	343.07
4d	250	125	31.25	125	269.75
4e	250	250	125	125	380.35
4f	250	250	250	250	320.27
4g	250	250	62.5	125	738.55
4h	31.25	125	125	62.5	55.26
4i	250	125	31.25	125	337.34
4j	62.5	125	125	125	253.81
4k	62.5	31.25	31.25	125	303.97
4l	31.25	125	62.5	62.5	292.12
4m	125	250	250	250	70.00
4n	125	250	250	250	308.24
4o	250	125	125	250	494.86
4p	250	250	62.5	125	469.95
4q	31.25	62.5	62.5	250	73.46
4r	15.62	62.5	31.25	62.5	95.33
4s	125	15.62	31.25	62.5	159.44
4t	31.25	125	62.5	62.5	131.52
4u	250	250	125	125	78.35
4v	7.81	62.5	15.62	31.25	59.33
4w	15.62	62.5	31.25	62.5	75.61
4x	62.5	31.25	31.25	125	174.4
Chloramphenicol	250	250	125	250	–
Ascorbic acid	–	–	–	–	33.70

3.4 | Antibacterial activity

The newly synthesized compounds (**4a–4x**) were tested for antibacterial activity against two Gram-positive and Gram-negative bacteria using the REMA. The antibacterial assay of the screened compounds (**4a–4x**) was investigated by MIC (Table 4). The antibacterial screening data revealed that the majority of the compounds exhibited the same and high activity against both Gram-positive and Gram-negative bacteria.

3.5 | Antioxidant activity by the DPPH method

The newly synthesized compounds (**4a–4x)** were tested for antioxidant activity by the DPPH method using ascorbic acid as standard. The antioxidant activity of standard and test compounds was estimated based on the radical scavenging effect of DPPH-free radical (Table 4). Most compounds are good antioxidants with more than 50% scavenging activity. Among them, the compounds **4h, 4m, 4n, 4q, 4u, 4v, and 4w** showed good radical scavenging activity while the remaining compounds showed moderate activity. The radical scavenging activity of α-aminophosphonates in the DPPH method increases with an increase in concentration. Comparable results were demonstrated by compounds **4h, 4m, 4q, 4u, 4v, and 4w** (half-maximal inhibitory concentration [IC_{50}] values of 55.26, 70.00, 73.46, 78.35, 59.33, and 75.61) with respect to standard ascorbic acid (IC_{50} = 33.70).

4 | CONCLUSION

The Ni-MOF was used as a heterogeneous catalyst for the synthesis of novel α-aminophosphonates under solvent-free condition. Ni-MOF seems to be an eco-friendly and an easily recyclable catalyst up to the eighth run without significant reduction in its catalytic activity. The synthesized α-aminophosphonates **4a–4x** were tested for their antibacterial (REMA) and antioxidant properties (DPPH). Compounds **4a–4x** exhibited excellent antibacterial activity in comparison with a reference drug, whereas compounds **4h, 4m, 4n, 4q, 4u, 4v, and 4w** showed better antioxidant activity compared with standard ascorbic acid. The synthesized compounds showed good antibacterial and antioxidant activities.

ACKNOWLEDGMENT

The authors are thankful to DST-PURSE, New Delhi, for awarding the research fellowship. The authors also acknowledge Microanalytical Laboratory and IRMRA (Thane) for providing characterization facilities.

ORCID

Navinchandra G. Shimpi https://orcid.org/0000-0003-0291-1804

REFERENCES

[1] G. Ferey, *Chem. Soc. Rev.* **2008**, *37*, 191.
[2] C. Janiak, *Dalton Trans.* **2003**, *14*, 2781.
[3] S. Kitagawa, R. Kitaura, S. Noro, *Angew. Chem. Int. Ed.* **2004**, *43*, 2334.
[4] M. C. Das, S. K. Ghosh, E. C. Sanudo, P. K. Bharadwaj, *Dalton Trans.* **2009**, *9*, 1644.
[5] M. P. Suh, H. J. Park, T. K. Prasad, D. Lim, *Chem. Rev.* **2012**, *112*, 782.
[6] Y. He, W. Zhou, G. Qian, B. Chen, *Chem. Soc. Rev.* **2014**, *43*, 5657.
[7] P. Horcajada, T. Chalati, C. Serre, R. Gref, *Nat. Mater.* **2010**, *9*, 173.
[8] M. Kurmoo, *Chem. Soc. Rev.* **2009**, *38*, 1353.
[9] P. Horcajada, C. Serre, G. Maurin, N. A. Ramsahye, F. Balas, M. V. M. Sebban, G. FereyFlexible, *J. Am. Chem. Soc.* **2008**, *130*, 6774.
[10] Y. Xiao, Y. Cui, Q. Zheng, S. Xiang, G. Qian, B. Chen, *Chem. Commun.* **2010**, *46*, 5503.
[11] A. H. Chughtai, N. Ahmad, H. A. Younus, A. Laypkov, F. Verpoort, *Chem. Soc. Rev.* **2015**, *44*, 6804.
[12] W. Dong, L. Zhang, C. Wang, C. Feng, N. Shang, S. Gao, C. Wang, *RSC Adv.* **2016**, *6*, 37118.
[13] A. Dhakshinamoorthy, A. M. Asiric, H. Garcia, *Chem. Soc. Rev.* **2015**, *44*, 1922.
[14] S. Maiti, T. Dhawa, A. Mallik, S. Mahanty, *Sustainable Energy Fuels* **2017**, *1*, 288.
[15] S. Aryanejad, G. Bagherzade, A. Farrokhi, *Appl. Organomet. Chem.* **2018**, *32*, 1.
[16] M. I. Kabachnik, T. Y. Medved, *Akademii Nauk SSSR.* **1952**, *83*, 689.
[17] E. K. Fields, *J. Am. Chem. Soc.* **1952**, *74*, 1528.
[18] I. E. Sayed, S. M. El Kosy, M. A. Hawata, M. M. A. El-Sattar, *J. American Science* **2011**, *7*, 357.
[19] K. M. Reddy, S. Santhisudha, G. Mohan, K. Peddanna, C. A. Rao, C. S. Reddy, *Phosphorus, Sulfur Silicon Relat. Elem.* **2016**, *191*, 933.
[20] B. Sujatha, S. Mohan, C. Subramanyam, K. P. Rao, *Phosphorus, Sulfur Silicon Relat. Elem.* **2017**, *192*, 1110.
[21] X. Huang, M. Wang, Y. Pan, X. Tian, H. Wang, Y. Zhang, *Bioorg. Med. Chem. Lett.* **2013**, *23*(19), 5283.
[22] J. Chen, W. Tang, J. Che, K. Chen, G. Yan, Y. Gu, D. Shi, *J. Agric. Food Chem.* **2015**, *63*(32), 7219.
[23] J. Hiratake, J. Oda, *Biasci. Biotech. Biochell.* **1997**, *61*(2), 211.
[24] S. A. Rasal, S. Jain, N. G. Shimpi, *Synth. Commun.* **2018**, *48*, 2420.
[25] S. A. Rasal, M. S. Tamore, N. G. Shimpi, *ChemistrySelect* **2019**, *4*, 2293.
[26] Y. K. Park, S. B. Choi, H. J. Nam, D. Jung, H. C. Ahn, K. Choi, H. Furukaw, J. Kim, *Chem. Commun.* **2010**, *46*, 3086.

[27] H. Zhao, H. Song, L. Chou, *Inorg. Chem. Commun.* **2012**, *15*, 261.
[28] Y. Ren, Y. Shi, J. Chen, S. Yang, C. Qi, H. Jiang, *RSC Adv.* **2013**, *3*, 2167.
[29] J. Canivet, S. Aguado, Y. Schuurman, D. Farrusseng, *J. Am. Chem. Soc.* **2013**, *135*, 4195.
[30] T. Truong, C. K. Nguyen, T. V. Tran, T. T. Nguyen, N. T. S. Phan, *Catal. Sci. Technol.* **2014**, *4*, 1276.
[31] W. Zuo, G. Yu, Z. Dong, *RSC Adv.* **2016**, *6*, 11749.
[32] K. Sel, S. Demirci, E. Meydan, S. Yildiz, O. F. Ozturk, H. AL-lohedan, N. Sahiner, *J. Electron. Mater.* **2015**, *44*(1), 136.
[33] J. C. Palomino, A. Martin, M. Camacho, H. Guerra, J. Swings, F. Portaels, *Antimicrob. Agents Chemother.* **2002**, *46*, 2720.
[34] M. S. Blois, *Nature* **1957**, *181*, 1199.
[35] G. Ruberto, M. T. Baratta, S. G. Deans, H. Dorman, *J. Planta Med.* **2000**, *66*, 687.
[36] J. M. Andrews, *J. Antimicrob. Chemother.* **2008**, *62*, 256.
[37] M. S. Blois, *Nature* **1958**, *26*, 1119.
[38] E. J. Gomez, L. Luyengi, S. K. Lee, L. F. Zhu, B. N. Zhou, J. M. Pezzuto, A. D. Kinghorn, *J. Nat. Prod.* **1998**, *26*, 706.
[39] J. Xu, C. Yang, Y. Xue, C. Wang, J. Cao, Z. Chen, *Electrochim. Acta* **2016**, *211*, 595.

SUPPORTING INFORMATION

Additional supporting information may be found online in the Supporting Information section at the end of this article.

How to cite this article: Rasal SA, Dhavan PP, Jadhav BL, Shimpi NG. Synthesis of new α-aminophosphonates using nanoscale nickel-based metal–organic framework as a heterogeneous catalyst and their antibacterial activity. *Appl Organometal Chem*. 2019;e5317. https://doi.org/10.1002/aoc.5317